Biogeosciences, 12, 2517–2531, 2015
www.biogeosciences.net/12/2517/2015/
doi:10.5194/bg-12-2517-2015

Biogeosciences Open Access

First on-line isotopic characterization of N_2O above intensively managed grassland

B. Wolf[1,2], L. Merbold[3], C. Decock[3], B. Tuzson[1], E. Harris[1], J. Six[3], L. Emmenegger[1], and J. Mohn[1]

[1]Laboratory for Air Pollution/Environmental Technology, Empa, Überlandstrasse 129, 8600 Dübendorf, Switzerland
[2]Institute for Meteorology and Climate Research (IMK-IFU), Karlsruhe Institute of Technology, Kreuzeckbahnstrasse 19, 82467 Garmisch-Partenkirchen, Germany
[3]Department of Environmental Systems Science, ETH Zurich, Universitätsstrasse 2, 8092 Zürich, Switzerland

Correspondence to: B. Wolf (benjamin.wolf@kit.edu)

Received: 9 December 2014 – Published in Biogeosciences Discuss.: 23 January 2015
Revised: 1 April 2015 – Accepted: 3 April 2015 – Published: 29 April 2015

Abstract. The analysis of the four main isotopic N_2O species ($^{14}N^{14}N^{16}O$, $^{14}N^{15}N^{16}O$, $^{15}N^{14}N^{16}O$, $^{14}N^{14}N^{18}O$) and especially the intramolecular distribution of ^{15}N ("site preference", SP) has been suggested as a tool to distinguish source processes and to help constrain the global N_2O budget. However, current studies suffer from limited spatial and temporal resolution capabilities due to the combination of discrete flask sampling with subsequent laboratory-based mass-spectrometric analysis. Quantum cascade laser absorption spectroscopy (QCLAS) allows the selective high-precision analysis of N_2O isotopic species at trace levels and is suitable for in situ measurements.

Here, we present results from the first field campaign, conducted on an intensively managed grassland site in central Switzerland. N_2O mole fractions and isotopic composition were determined in the atmospheric surface layer (at 2.2 m height) at a high temporal resolution with a modified state-of-the-art laser spectrometer connected to an automated N_2O preconcentration unit. The analytical performance was determined from repeated measurements of a compressed air tank and resulted in measurement repeatability of 0.20, 0.12 and 0.11 ‰ for $\delta^{15}N^{\alpha}$, $\delta^{15}N^{\beta}$ and $\delta^{18}O$, respectively. Simultaneous eddy-covariance N_2O flux measurements were used to determine the flux-averaged isotopic signature of soil-emitted N_2O.

Our measurements indicate that, in general, nitrifier-denitrification and denitrification were the prevalent sources of N_2O during the campaign and that variations in isotopic composition were due to alterations in the extent to which N_2O was reduced to N_2 rather than to other pathways, such as hydroxylamine oxidation. Management and rewetting events were characterized by low values of the intramolecular ^{15}N site preference (SP), $\delta^{15}N^{bulk}$ and $\delta^{18}O$, suggesting that nitrifier-denitrification and incomplete heterotrophic bacterial denitrification responded most strongly to the induced disturbances. The flux-averaged isotopic composition of N_2O from intensively managed grassland was 6.9 ± 4.3, -17.4 ± 6.2 and 27.4 ± 3.6 ‰ for SP, $\delta^{15}N^{bulk}$ and $\delta^{18}O$, respectively. The approach presented here is capable of providing long-term data sets also for other N_2O-emitting ecosystems, which can be used to further constrain global N_2O inventories.

1 Introduction

Atmospheric nitrous oxide (N_2O) mole fraction has been increasing since preindustrial times, predominately due to increased agricultural activity (Davidson, 2009; Mosier et al., 1998). Owing to the approximately 300 times higher global warming potential (GWP) compared to CO_2, this greenhouse gas (GHG) currently accounts for 6 % of total anthropogenic radiative forcing (Myhre et al., 2013). Recent estimates showed that N_2O is, in addition, the single most important ozone-depleting substance (Ravishankara et al., 2009). Because at least 60 % of total anthropogenic N_2O emissions are attributed to food production (Syakila and Kroeze, 2011), a growing human population and meat consumption per capita as well as biofuel production will accelerate the rate of increase in atmospheric N_2O concentration. Hence, the de-

velopment of adequate mitigation strategies is pertinent and requires a better understanding of the processes driving N_2O fluxes. To date, nitrification, nitrifier-denitrification and denitrification are considered to constitute the dominant N_2O-producing processes, especially in agricultural soils (Wrage et al., 2001). Other N_2O source processes such as abiotic N_2O production, co-denitrification and heterotrophic nitrification have also been observed; a concise overview of observed processes is given elsewhere (Butterbach-Bahl et al., 2013). This complexity inherent in the N cycle and associated transformation processes is a major challenge in developing mitigation strategies, as the attribution of N_2O production to the respective processes is required to tailor target-oriented actions (Baggs, 2008). Approaches for apportioning N_2O emissions to nitrification and denitrification and N_2O reduction to N_2 (source partitioning) have mostly relied on acetylene (C_2H_2) inhibition and isotope labeling (Groffman et al., 2006), but denitrification rates are underestimated by the C_2H_2 method (Butterbach-Bahl et al., 2013; Groffman et al., 2006; Watts and Seitzinger, 2000). Isotope labeling approaches are vulnerable to incomplete diffusion of the tracer and to the stimulation of process rates by the addition of the labeled substrates themselves (Groffman et al., 2006). Changes in the natural abundance of ^{15}N and ^{18}O in N_2O have been explored to investigate N_2O production processes, but the $\delta^{15}N$ and $\delta^{18}O$ determined depend on both fractionation factors and the isotopic composition of precursors, which in turn exhibit strong variations (Baggs, 2008; Bedard-Haughn et al., 2003; Heil et al., 2014; Toyoda et al., 2011).

N_2O is a linear molecule and four main isotopic species can be discerned: $^{14}N^{14}N^{16}O$, $^{14}N^{15}N^{16}O$, $^{15}N^{14}N^{16}O$ and $^{14}N^{14}N^{18}O$. The isotopic species $^{14}N^{14}N^{16}O$, $^{14}N^{14}N^{18}O$ and $^{14}N^{15}N^{16}O$ (or $^{15}N^{14}N^{16}O$) are isotopologues, while $^{14}N^{15}N^{16}O$ and $^{15}N^{14}N^{16}O$ are isotopomers and will be termed $^{15}N^{\alpha}$-N_2O and $^{15}N^{\beta}$-N_2O (Toyoda and Yoshida, 1999). The umbrella term isotopocule is used for both isotopomers and isotopologues. The intramolecular distribution of ^{15}N in N_2O ("site preference"; $SP = \delta^{15}N^{\alpha} - \delta^{15}N^{\beta}$) has been reported to be independent of the substrate's isotopic composition, as SP in the N_2O produced de novo remained constant even though $\delta^{15}N$ and $\delta^{18}O$ values of both N_2O and substrates changed markedly during experiments with pure cultures (Heil et al., 2014; Sutka et al., 2003, 2006, 2008; Toyoda et al., 2005). Therefore, SP can be considered as a tracer conserving the source process information (Ostrom and Ostrom, 2011). The SP of different processes has been characterized in a number of pure-culture, mixed-culture (Ostrom et al., 2007; Sutka et al., 2003, 2006; Toyoda et al., 2005; Wunderlin et al., 2012, 2013) and soil-incubation studies (Köster et al., 2011, 2013a; Lewicka-Szczebak et al., 2014; Well et al., 2006, 2008), with a compilation of data in Toyoda et al. (2011). A recent review on source partitioning and SP (Decock and Six, 2013b) concluded that SP is capable of distinguishing between the process groups N_2O_N (NH_2OH oxidation, fungal denitrification and abiotic N_2O production; $SP = 32.8 \pm 4.0$ ‰) and N_2O_D (nitrifier-denitrification and denitrification; $SP = -1.6 \pm 3.8$ ‰). In addition, N_2O isotopocules can be used as an independent validation of the global, measurement-based bottom-up N_2O budget and have already confirmed that the isotopically light sources such as agriculture and industry contribute to the increase in atmospheric N_2O (Toyoda et al., 2013; Yoshida and Toyoda, 2000). Owing to the temporal and spatial variability of isotopomer ratios, it is indispensable to derive flux-weighted average values from different sources (such as ecosystems) for later use in budget analysis using box models (Kim and Craig, 1993; Perez et al., 2001; Yoshida and Toyoda, 2000).

N_2O isotopomers can be measured by mass spectrometry, but this requires discrete flask sampling with subsequent laboratory analysis. Hence, this approach is limited in temporal resolution and spatial representation of a given site. Additionally, it is indirect, as information on the site-specific isotopic composition is derived from the analysis of the NO^+ fragment and N_2O^+ molecular ion. Recently, a quantum cascade laser absorption spectrometer (QCLAS) capable of selective analysis of the three most abundant N_2O isotopocules has been presented (Waechter et al., 2008), and its potential for in situ measurements in conjunction with an automated pre-concentration unit has been shown (Mohn et al., 2010, 2012). Here we present the results obtained from a, to our knowledge first, campaign in which the isotopic composition of N_2O (SP, $\delta^{15}N$, $\delta^{18}O$) in the atmospheric surface layer was determined on-line by using an optimized state-of-the-art laser spectrometer. Using the combination of N_2O isotopic analysis by QCLAS, accompanying eddy-covariance-based N_2O flux measurements as well as the monitoring of environmental conditions and inorganic nitrogen concentrations, our specific objectives for this study were (i) to demonstrate the capability of QCLAS systems for carrying out high-precision isotopic analysis of (soil-emitted) N_2O in ambient air; (ii) to investigate management and weather effects on isotopic composition and source processes; and (iii) to characterize the flux-averaged isotopic composition of N_2O emitted from an intensively managed grassland site.

2 Material and methods

2.1 Study site

The agricultural research station Chamau (CHA) is located in central Switzerland at an elevation of 400 m a.s.l. The experiment was conducted on intensively managed grassland belonging to CHA which is primarily used for fodder production and occasional winter grazing by sheep (Zeeman et al., 2010). The soil type is a Cambisol with a bulk density of 0.97 g cm^{-3}, 30.6 % sand, 47.7 % silt and 21.8 % clay in the top 10 cm and pH of 5.7–6.2. Soil carbon and nitrogen con-

Table 1. Reference gas and compressed air tanks used during the campaign. S1 and S2 represent the anchor and calibration standard. C1 and C2 are the target gases used for determination of system performance. The reported precision is 1σ.

Tank	$\delta^{15}N^{\alpha}$ (‰)	$\delta^{15}N^{\beta}$ (‰)	$\delta^{18}O$ (‰)	$\delta^{15}N^{bulk}$ (‰)	SP (‰)	mixing ratio (ppm)/(ppb)*
S1	15.66 ± 0.03	-3.22 ± 0.13	34.89 ± 0.05	6.22 ± 0.07	18.88 ± 0.13	90.09 ± 0.01
S2	10.38 ± 0.03	-10.55 ± 0.1	25.44 ± 0.06	-0.09 ± 0.05	20.93 ± 0.10	87.28 ± 0.003
C1	15.40 ± 0.08	-3.04 ± 0.06	43.65 ± 0.08	6.18 ± 0.05	18.44 ± 0.10	327.01 ± 0.05
C2	15.65 ± 0.17	-4.27 ± 0.08	44.20 ± 0.07	5.69 ± 0.09	19.92 ± 0.19	327.45 ± 0.05

* ppm for S1 and S2, ppb for C1, C2.

tent in the top 10 cm was 37.9 and 4.1 g kg^{-1} (Roth, 2006). Mean annual temperature and annual precipitation are 9.1 °C and 1151 mm, respectively (Zeeman et al., 2010). Management practices aim at fodder production and consist of mowing followed by slurry application, with up to six mowing and slurry applications per year and the occasional grazing of sheep and cattle in October and November. During the campaign in summer 2013, three management cycles were carried out. Harvest dates were 6 June, 11 July and 21 August, and slurry was applied within 10 days after each mowing event. Nitrogen input was calculated from the amount of slurry applied to the field and the N concentration determined (Labor für Boden- und Umweltanalytik, Eric Schweizer AG, Thun, Switzerland) in a sample drawn from the supply to the trailing hose applicator. The applied N amounted to 30, 40 and 43.3 kg N ha^{-1} for the first, second and third application, respectively. Grassland is reestablished via ploughing and resowing approximately every 10 years. The last reestablishment event took place in 2012 (Merbold et al., 2014).

2.2 Instrumental setup for analysis of N_2O isotopocule ratios

The four most abundant N_2O isotopic species were quantified using a modified QCLAS (Aerodyne Research Inc., Billerica MA, USA) equipped with a continuous-wave quantum cascade laser (cw-QCL) with spectral emission at 2203 cm^{-1}, an astigmatic Herriott multi-pass absorption cell (204 m path length, AMAC-200) and a reference path with a short (5 cm) N_2O-filled cell to lock the laser emission frequency (Tuzson et al., 2013). During the campaign, the QCLAS was operated in an air-conditioned trailer located 60 m west of the eddy-covariance (EC) tower. This trailer position contributes < 20 % to the main flux and is at the far side of the prevailing wind direction (Zeeman et al., 2010). The sample air inlet was installed next to the inlet of the EC tower (2.2 m height). Sample air was drawn through a PTFE tube (4 mm ID) by a membrane pump (PM 25032-022, KNF Neuberger, Switzerland). Upstream of the pump, the sample air was pre-dried with a permeation drier (MD-050-72S-1, PermaPure Inc., USA). Following the pump, the pressure was maintained at 4 bar overpressure using a pressure relief valve. Humidity as well as CO_2 were quantitatively removed from the gas flow by applying a chemical trap filled with Ascarite (7 g, 10–35 mesh, Fluka, Switzerland) bracketed by $Mg(ClO_4)_2$ (2×1.5 g, Fluka, Switzerland). Finally, the sample gas was passed through a sintered metal filter (SS-6F-MM-2, Swagelok, USA) and directed to a preconcentration unit described in detail previously (Mohn et al., 2010, 2012). For an increase in N_2O mixing ratios from ambient level to around 50 ppm N_2O, approx. 8 L of ambient air were preconcentrated. Afterwards, the preconcentrated N_2O was introduced into the evacuated multi-pass cell of the QCLAS. Isotopic fractionation during preconcentration (increase by 0.31 ± 0.10, 0.34 ± 0.16 and 0.29 ± 0.07 ‰ for $\delta^{15}N^{\alpha}$, $\delta^{15}N^{\beta}$ and $\delta^{18}O$, respectively) was quantified by the preconcentration of N_2O with a known isotopic composition and subsequently corrected. The compatibility of N_2O isotopomer analysis by QCLAS with isotope ratio mass spectrometry (IRMS) laboratories was recently demonstrated in an inter-laboratory comparison campaign (Mohn et al., 2014).

2.3 Measurement and calibration strategy

To ensure high accuracy and repeatability of the analytical system, a measurement and calibration strategy similar to the one presented by Mohn et al. (2012) was applied. It is based on two standard gases differing in N_2O isotopic composition, which were produced by the dynamic dilution of pure medical N_2O (Pangas, Switzerland) with defined amounts of isotopically pure (> 98 %) $^{14}N^{15}N^{16}O$ (Cambridge Isotope Laboratories, USA) and (> 99.95 %) $^{14}N^{14}NO$ (ICON Services Inc., USA). Subsequent gravimetric dilution with high-purity synthetic air (99.999 %, Messer Schweiz AG) resulted in pressurized gas mixtures with 90 ppm N_2O (10^{-6} moles of trace gas per mole of dry air). Both standards were calibrated against primary standards which were previously measured by the Tokyo Institute of Technology (TIT, Toyoda and Yoshida) to anchor δ values to the international isotopic standard scales. The first standard (S1, Table 1) was used as an anchor point to the international δ scale and used as input data for data analysis algorithms (see data processing). Therefore, the N_2O isotopic composition of S1 was tar-

Table 2. Adjusted r^2 and p values for regression analysis of Keeling-plot-derived isotopic compositions in soil-emitted N_2O versus auxiliary variables N_2O flux (f_{N_2O}), difference of maximum and minimum concentration over a noon-to-noon period (ΔN_2O), precipitation (prcp), soil moisture (wfps), and nutrient concentrations (NO_3^-, NH_4^+ and DOC).

Explanatory	SP r^2	SP p	$\delta^{15}N^{bulk}$ r^2	$\delta^{15}N^{bulk}$ p	$\delta^{18}O$ r^2	$\delta^{18}O$ p	N
f_{N_2O}	0.14	**	0.04	0.06	0.16	**	62
ΔN_2O	0.09	*	0.1	*	0.11	*	65
prcp	0.24	**	0.03	0.08	0.24	**	62
wfps	0.14	*	0.29	**	−0.009	0.52	65
T	0.22	**	0.30	**	0.12	*	65
DOC	0.23	*	0.30	*	0.03	0.23	18
NO_3^-	0.04	0.14	0.27	*	0.16	*	31
NH_4^+	−0.03	0.75	−0.03	0.89	−0.03	0.93	31

Significance codes: * $p < 0.05$; ** $p < 0.001$. Sample size (n) differs due to data availabilities.

geted to closely resemble background air. As the N_2O isotopic composition of surface layer air is mainly a mixture of soil-derived and background composition, the second standard (S2, Table 2) used for span correction was depleted in $\delta^{15}N^{\alpha}$, $\delta^{15}N^{\beta}$ and $\delta^{18}O$ compared to background air in accordance with the expected terrestrial source signatures.

The measurement protocol started with the injection of S1, dynamically diluted to 50 ppm, the mole fraction of ambient N_2O after preconcentration. After flushing the absorption cell with synthetic air, S2 was injected and also diluted to 50 ppm. For the determination of the slight concentration dependence already reported (Mohn et al., 2012), S1 was injected again but at a higher mole fraction of 67 ppm (later referred to as $S1_h$). This mole fraction represents the mole fraction expected after the preconcentration of high-concentration surface layer air. Subsequently, S1 was injected again and diluted to 50 ppm, before the cell was filled with preconcentrated ambient N_2O (A). This subroutine (S1 + A) of injection of S1 and preconcentrated ambient N_2O took 35 min and was repeated three times. For an independent determination of repeatability, the fourth sample was preconcentrated compressed air (target gas). During the campaign, two compressed air cylinders (C1 and C2, referred to as target gas) were used. The isotopic composition and N_2O mixing ratio of both cylinders were determined in the laboratory prior to the campaign start (Table 1). N_2O mole fractions and isotopic composition analyzed in the laboratory and at the field site agreed within their analytical uncertainty. Following target gas analysis, S1 and $S1_h$ were analyzed again. Another set of three subroutines S1+A completed one run. One complete cycle of 6 ambient air samples and one compressed air sample took 340 min, leading to approx. 25 ambient air samples being analyzed during 24 h. N_2O mole fractions were determined according to Mohn et al. (2012).

2.4 Data processing

Data processing is based on individual mixing ratios of the four main N_2O isotopic species and spectrometer characteristics as recorded by the instruments's software (TDLWintel, Aerodyne Research Inc., Billerica, MA, USA). In the first step, variations in the isotope ratios induced by drifts in the instrument working parameters during the field operation were corrected. A linear additive model explaining the deviation of isotope ratios R^{α}, R^{β} and R^{18O} for repeated measurements of standard S1 from their mean value by absorption cell temperature ($T1$), laser temperature ($T2$), line position (LP) and pressure (p) was calibrated based on S1 injections. For isotope ratios of S1, $S1_h$, S2, sample air and compressed air, these systematic deviations were corrected based on the respective values of $T1$, $T2$, LP and p. In a second step, concentration dependence of isotope ratios, determined using the measurements of S1 and $S1_h$, was addressed with corrections (0.013, 0.028 and 0.004 ‰ ppb^{-1} for $\delta^{15}N^{\alpha}$, $\delta^{15}N^{\beta}$ and $\delta^{18}O$) being in the same range as described earlier (Mohn et al., 2012). Subsequently, remaining drifts were corrected based on the analysis of S1. Finally, isotope ratios were converted to δ values using a two-point calibration derived from corrected values of S1 and S2.

2.5 Determination of soil-emitted N_2O isotopic composition

The isotopic composition of the source process "soil N_2O emission" was derived using the Keeling plot approach (Keeling, 1958), where δ values measured (here at 2.2 m height) are plotted versus the inverse of N_2O mole fractions. The intercept of the linear regression line can be interpreted as the isotopic composition of soil-emitted N_2O (Pataki et al., 2003). Therefore, the determination of soil N_2O isotopic composition requires an increase in N_2O mole fraction. During the day, turbulence mixes surface layer air into the at-

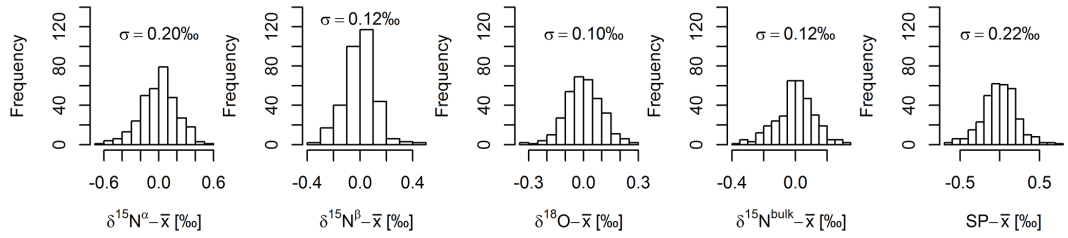

Figure 1. Long-term stability (standard deviation σ) derived by target gas injections ($n = 331$) over a 3-month period. As two target gas tanks were used, histograms show deviation of respective tank means, $\bar{x}$, for $\delta^{15}N^{\alpha}$, $\delta^{15}N^{\beta}$, $\delta^{18}O$, $\delta^{15}N^{bulk}$ and SP.

mospheric background. At night, the surface layer becomes more stable and the N_2O mole fraction increases, shifting isotopic composition towards its source composition. As a consequence, Keeling plots were based on noon-to-noon periods. This approach is discussed in Sect. 4.6.

2.6 N_2O flux measurement

At CHA, greenhouse gas mole fractions, including N_2O, have been measured continuously since 2012 by means of the EC method (Baldocchi and Meyers, 1998). The system consists of a three-dimensional sonic anemometer to measure wind speed and direction (2.41 m height, Solent R3, Gill Instruments, Lymington, UK) and a QCLAS (mini-QCLAS, Aerodyne Research Inc., Billerica, MA, USA) to determine N_2O mole fractions at a temporal resolution of 10 Hz. Both data streams are merged in near real time within a data acquisition system (MOXA embedded Linux computer; Moxa, Brea, CA, USA) via an RS-232 serial data link (Eugster and Plüss, 2010). The setup has been described in detail previously (Merbold et al., 2014). Post-processing of N_2O fluxes included screening for obvious out-of-range values ($\pm 100\,\mathrm{nmol\,m^{-2}\,s^{-1}}$). N_2O fluxes were further aggregated to noon-to-noon daily averages to smoothen the large variability in the 30 min flux averages. Daily averages were calculated for days where more than 30 half-hour values were available, with this filter excluding 3 days from analysis.

2.7 Soil inorganic N, dissolved organic C and environmental conditions

Ammonium (NH_4^+) and nitrate (NO_3^-) concentrations were determined from soil (0–20 cm depth) sampled at 10 positions along a transect within the footprint of the EC measurements following the predominant wind direction. Samples were taken weekly throughout the campaign or daily during mowing and slurry application events. Per sample, ~ 15 g of fresh soil were added to specimen vessels containing 50 mL 1 M KCl. After 1 h on a shaker, the supernatant was filtered (Whatman no. 42 ashless filter paper, 150 mm diameter) and analyzed colorimetrically for NH_4^+ and NO_3^-. For a subset of extracts, we determined dissolved organic carbon (DOC) concentrations by combustion of KCl extracts using a total organic C analyzer (Shimdazu TOC-V, Columbia, MD, USA).

Soil temperatures and volumetric soil moisture contents at 10 cm depth were measured at the same 10 locations along the transect (5TM-sensors, Decagon Devices Ltd., Pullman, USA). Data were stored as 10 min averages on a data logger (EM50, Decagon Devices Ltd., Pullman, USA). The volumetric water content was converted to water-filled pore space (wfps) using a bulk density of $1.09\,\mathrm{g\,cm^{-3}}$. Precipitation was measured with a tipping bucket rain gauge (Type 10116, Toss GmbH, Potsdam, Germany) and stored as 10 min averages on a data logger (CR10X-2M, Campbell Scientific Inc., Logan, USA).

3 Results

3.1 Long-term precision for target gas analysis

System performance for N_2O mole fractions and isotopic composition was determined based on the repeated analysis of compressed air from target gas tanks (C1, C2). There was no significant drift in the δ values and N_2O mole fractions, indicating the stability of the applied measurement technique. Repeatability, calculated as the standard deviation (σ) of 331 target gas measurements, amounted to 0.20, 0.12, 0.10, 0.12 and 0.22 ‰ for $\delta^{15}N^{\alpha}$, $\delta^{15}N^{\beta}$, $\delta^{18}O$, $\delta^{15}N^{bulk}$ and SP, respectively (Fig. 1). The standard deviation for the N_2O mole fraction of the target gas was 0.25 ppb.

3.2 N_2O mole fractions and isotopic composition at 2.2 m height

Air samples were taken at 2.2 m height, which is within the lowest 10 % of the atmospheric boundary layer (ABL) where mechanical generation of turbulence exceeds buoyant generation or consumption. This part of the ABL is called surface layer; hence, corresponding air samples are referred to as surface layer air samples. N_2O isotopic composition of the surface layer air samples ($n = 2130$) ranged from 2.5 to 16.1 ‰, −11.9 to −2.4 ‰, 37.6 to 44.6 ‰, −4.6 to 6.6 ‰ and 14.3 to 19.3 ‰ for $\delta^{15}N^{\alpha}$, $\delta^{15}N^{\beta}$, $\delta^{18}O$, $\delta^{15}N^{bulk}$ and SP, respectively (Fig. 2). Surface layer N_2O mole fractions varied between 325 and 469 ppb and followed a diurnal cycle with

highest values during the night, when the boundary layer became more stable. Increasing N_2O mole fractions were associated with decreasing δ values, indicating that soil-emitted N_2O that was mixed into the surface layer was depleted in ^{15}N as compared to N_2O in the atmospheric background.

3.3 Auxiliary measurements

Half-hourly N_2O fluxes were averaged from noon-to-noon (f_{N_2O}) and ranged from -1 to 5 nmol m^{-2} s^{-1}. Maximum N_2O fluxes coincided with an overnight build up in N_2O mole fractions (ΔN_2O) as analyzed by QCLAS and could not be attributed to slurry application events alone (Fig. 3). Among the correlations of f_{N_2O} and auxiliary variables, only the one with a nitrate concentration ($r^2 = 0.18$) was significant ($p < 0.01$). Soil water content (wfps) was modulated by precipitation, and two clear states could be identified. During the "wet" part of the campaign, lasting until 7 July, average wfps was 62 ± 4 % and thus was significantly (t test, $p < 0.001$) higher than the average of 37 ± 4 % calculated for the remainder of the campaign (referred to as the "dry" part). Soil temperature did not show such a clear two-phase pattern; however, temperatures during the first, wet part were 16.7 ± 4 °C and thus significantly ($p < 0.001$) lower than during the dry phase (21.2 ± 2 °C).

Background NH_4^+ and NO_3^- concentrations were smaller than 3 µg g_{soil}^{-1} and clearly responded to mowing and slurry application in the second and third management events. The NO_3^- concentration was higher than the NH_4^+ concentration and peaked at 16 and 50 µg g_{soil}^{-1}, while NH_4^+ concentration peaked at 9 and 15 µg g_{soil}^{-1} for these two management events. In contrast, dissolved organic carbon concentrations (DOC) did not respond to management events but were higher during the dry phase of the campaign ($p < 0.001$).

3.4 Isotopic composition of soil-emitted N_2O

The uncertainty of the determined source isotopic composition was estimated based on the standard error of the Keeling plot intercept and depends on the degree to which soil air accumulates in the surface layer (ΔN_2O, Fig. 4). For instance, the intercept (source) standard error ranged from 0.3 to 82 ‰ for SP. To apply the Keeling plot approach only to situations in which soil air accumulated in the surface layer, only source isotopic compositions for overnight increases in N_2O mole fractions of more than 12 ppb were considered in this study. This filter led to a maximum and average (μ) standard error of 6.8 ($\mu = 2.2$) ‰, 4.5 ($\mu = 1.4$) ‰ and 2.2 ($\mu = 1$) ‰ for SP, $\delta^{15}N^{bulk}$ and $\delta^{18}O$ isotopic source signatures, respectively.

During the field campaign, the Keeling-plot-derived isotopic composition of soil-emitted N_2O ranged from 1.4 to 17.3 ‰, -29 to -3 ‰ and 22.6 to 34.8 ‰ for SP, $\delta^{15}N^{bulk}$ and $\delta^{18}O$, respectively. All explanatory variables except NH_4^+ and NO_3^- were found to significantly correlate with

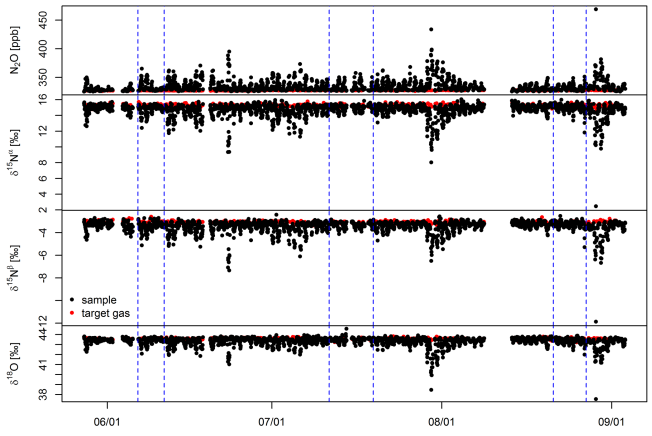

Figure 2. Target gas (red) and surface layer (black) N_2O mole fractions (top) and δ values (three bottom panels) measured in the atmospheric surface layer at 2.2 m height during the field campaign. Each pair of vertical dashed blue lines indicates the management events mowing (first line) and fertilization (second line).

SP (Table 2). For $\delta^{15}N^{bulk}$, correlations with ΔN_2O, wfps, soil temperature, DOC and NO_3^- and for $\delta^{18}O$ correlations of f_{N_2O}, ΔN_2O, precipitation, soil temperature and NO_3^- were significant. However, the adjusted r^2 for all regressions was below 0.4; in addition, multiple explanatory variables such as NH_4^+ and NO_3^- or wfps and temperature (Fig. 5) did not increase the explained variance above this value.

3.5 Event-based data aggregation

As already described in the section "Auxiliary measurements", there was a wet phase ($n = 27$ Keeling-plot-derived N_2O isotopic compositions) in the beginning of the campaign, which lasted about 1 month, and a dry phase lasting about 2 months ($n = 38$). Therefore, the data set was split into two corresponding parts with averages of 7.4 ± 3.6 vs. 11.1 ± 4.2 ‰ for SP, -19 ± 3.8 vs. -12.5 ± 5.9 ‰ for $\delta^{15}N^{bulk}$ and 28.7 ± 2.2 vs. 29.7 ± 3.4 ‰ for $\delta^{18}O$ in the wet vs. the dry phase, respectively. Averages of SP and $\delta^{15}N^{bulk}$ were significantly different ($p < 0.001$), but $\delta^{18}O$ averages were not. Based on this simple classification, the dry phase contains rewetting events. A rewetting event was defined as a 2-day period starting at the day for which wfps increased. Exclusion of these rewetting events during the dry phase increased average δ values ($n = 30$) and decreased standard deviations for SP, $\delta^{15}N^{bulk}$ and $\delta^{18}O$ to 12.5 ± 3.4, -10.8 ± 4.5 and 30.7 ± 2.8 ‰ . Moreover, the difference in $\delta^{18}O$ was significant ($p < 0.001$).

In addition to the dry/wet classification, we also defined three subsets representing the N_2O emission associated with the management events of mowing followed by fertilization ("Mana I"–"Mana III"), one subset representing a rewetting event between Mana II and III ("Rewetting") and one subset representing background ("BG", all remaining measure-

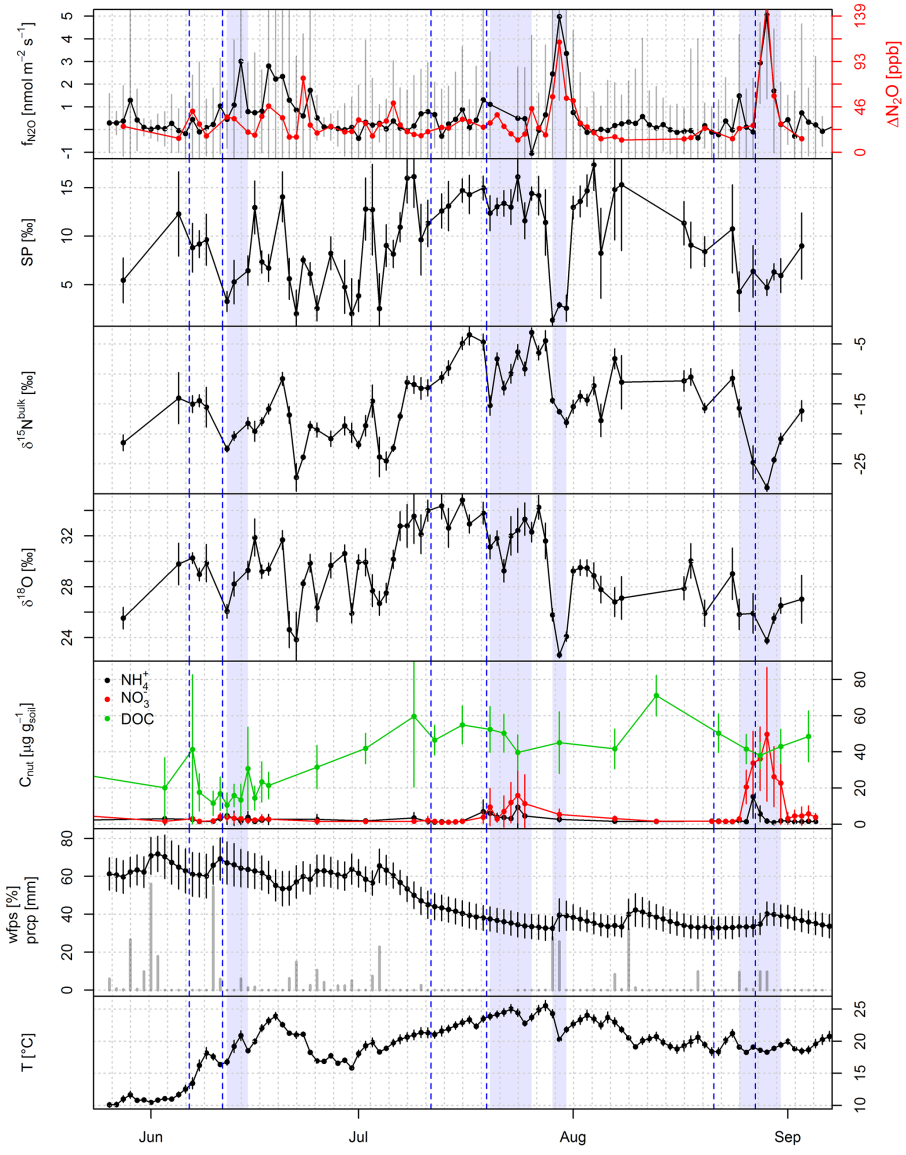

Figure 3. Noon-to-noon averaged N_2O flux (f_{N_2O}), overnight increase in N_2O mole fractions (difference in minimum and maximum N_2O concentration in a noon-to-noon period; ΔN_2O), Keeling-plot-derived isotopic composition of soil-emitted N_2O (SP, $\delta^{15}N^{bulk}$, $\delta^{18}O$), nutrient concentrations (ammonium, nitrate and dissolved organic carbon; DOC), water-filled pore space (wfps), precipitation (prcp) and soil temperature (T) over the measurement period. Each pair of vertical dashed blue lines indicates the management events mowing (first line) and fertilization (second line). Transparent blue sections represent periods of N_2O emission influenced by management or rewetting (third section).

ments). There were two distinct rewetting events between management events II and III, but N_2O isotopic composition is only available for the first one (29–31 July 2014). Isotopic compositions of soil-emitted N_2O were assigned to subsets of management or rewetting if the associated flux or nutrient concentration was elevated. This classification scheme led to 3 to 7 measurements for management and rewetting events (Fig. 3, underlaid in blue), while 47 measurements were assigned to class BG. Boxplots for SP, $\delta^{15}N^{bulk}$, $\delta^{18}O$ and wfps (Fig. 6) showed characteristic δ values and wfps for management and rewetting but not for subset BG. Measurements assigned to BG covered practically the whole range of values observed across all the other classes. Therefore, standard deviations for class BG were 1 order of magnitude larger than for the four other classes.

Statistical analysis is confounded by low and unequal sample size, so we compared exclusively the subsets management and rewetting using multiple nonparametric Wilcoxon tests after having checked the homogeneity of variances us-

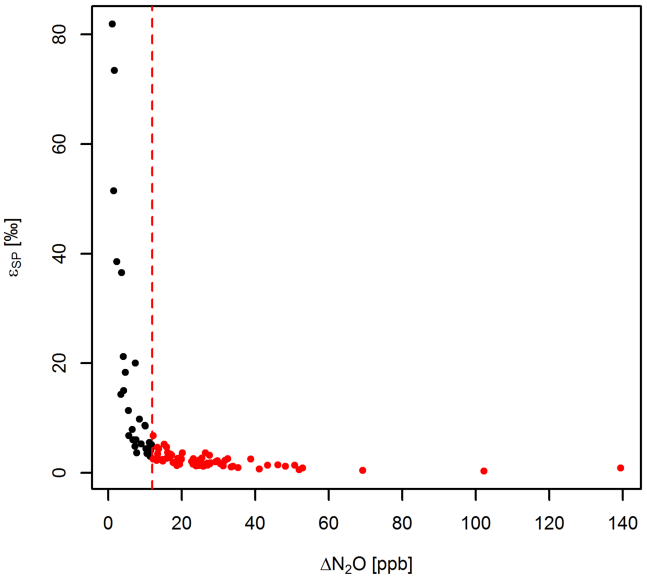

Figure 4. Standard error for SP (ε_{SP}) of soil-derived N_2O estimated by the Keeling plot approach as function of overnight N_2O accumulation in the surface layer. The red dashed line shows 12 ppb increase in N_2O mole fractions. Red dots represent the selected subset.

ing the Bartlett test. For all investigated δ values, only differences between groups Mana II and Mana III were significant.

3.6 Averages of N_2O isotopic signature for intensively managed grassland

Simple averages of the daily isotopic composition of soil-emitted N_2O were 9.6 ± 4.4, -15.2 ± 6.0 and 29.3 ± 3 ‰ for SP, $\delta^{15}N^{bulk}$ and $\delta^{18}O$, respectively ($n = 62$). Representative isotopic composition of N_2O emitted from a given site or treatment can be estimated based on flux-weighted averages of daily isotopic composition. For some noon-to-noon periods included in the above average, thus including an overnight increase in N_2O mole fractions of at least 12 ppb, negative N_2O fluxes were detected by the EC system (-0.17 ± 2.1 nmol m^{-2} s^{-1}; $n = 14$). This might be due to the uncertainty of N_2O flux measurements, temporal averaging over positive and negative fluxes in a noon-to-noon period, or different footprint regions for N_2O flux and isotopic analysis (flux vs. concentration footprint). To avoid bias in the flux-weighted average of emitted N_2O due to either one of the abovementioned possible reasons, the weighted averages were calculated for positive flux events only. Flux-weighted averages were 6.9 ± 4.3, -17.4 ± 6.2 and 27.4 ± 3.6 ‰ for SP, $\delta^{15}N^{bulk}$ and $\delta^{18}O$, respectively ($n = 48$).

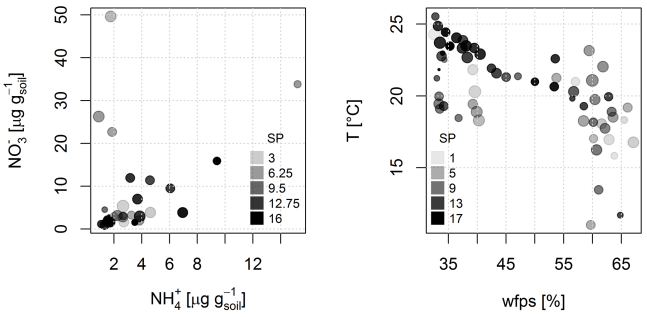

Figure 5. Maps of SP in relation to NH_4^+ and NO_3^- and SP in relation to wfps and soil temperature. The size of the points is inversely scaled to Keeling plot intercept standard error so that biggest points are those with lowest uncertainty.

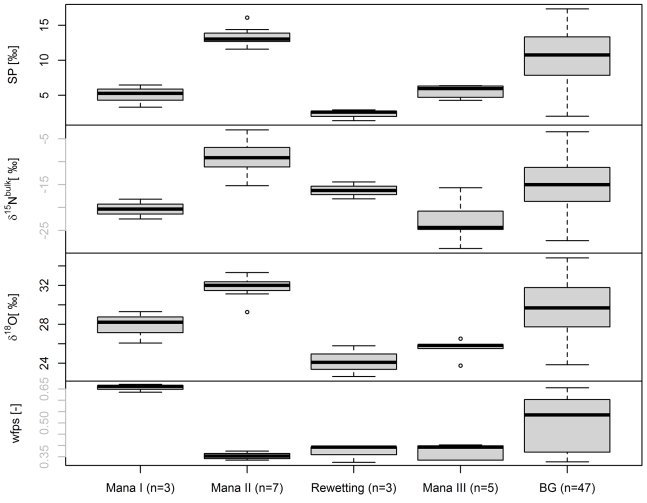

Figure 6. Boxplots for Keeling-plot-derived SP, $\delta^{15}N^{bulk}$, $\delta^{18}O$ of soil-emitted N_2O and wfps of management events (Mana I–III), rainfall after a dry period (Rewetting) and the remaining measurement period (BG).

4 Discussion

4.1 Analytical performance

To our knowledge, only two pilot studies exist demonstrating the potential of QCLAS-based analytical techniques for on-line and high-precision analysis of N_2O mole fractions and isotopic composition in surface layer air. While Mohn et al. (2012) analyzed the three most abundant ^{15}N isotopocules ($^{14}N^{14}N^{16}O$, $^{15}N^{14}N^{16}$, $^{14}N^{15}N^{16}O$), Harris et al. (2014) included the ^{18}O isotopologue ($^{14}N^{14}N^{18}O$). In both studies, however, the instrument was located in the laboratory. Based on 3 weeks of measurements, Mohn et al. (2012) reported a precision of 0.24 and 0.17 ‰ for $\delta^{15}N^{\alpha}$ and $\delta^{15}N^{\beta}$, respectively, and Harris et al. (2014) reported 0.17, 0.19 and 0.32 ‰ for $\delta^{15}N^{\alpha}$, $\delta^{15}N^{\beta}$ and $\delta^{18}O$, respectively, for a 12-day period. In both studies, in accordance with the present study, ana-

lytical performance was determined based on the repeated analysis of compressed air samples. Thereby, the analytical precision reached in the present study was distinctly higher for $\delta^{15}N^{\beta}$ and $\delta^{18}O$ and similar for $\delta^{15}N^{\alpha}$ compared to these two previous studies, even though the measurements were done under field conditions and over a much longer, 3-month, period. This confirms the high level of precision associated with the QCLAS-based determination of N_2O isotopic composition. Standard errors for Keeling plot intercepts (Fig. 4) confirm that this precision is sufficient to resolve the variability of atmospheric N_2O sampled close to the ground. As our instrument was located directly at the field site and measurements were conducted over a period of more than 3 months, our study indicates that this level of repeatability can be achieved both on long timescales and in the field.

4.2 N_2O isotopic composition in the atmospheric surface layer (2.2 m height)

In our study, δ values of single preconcentrated air samples were between atmospheric background and 14.3 ‰ (SP) and −4.7 ‰ ($\delta^{15}N^{bulk}$). Mohn et al. (2012) reported similar values between atmospheric background and 12 ‰ (SP) and −4 ‰ ($\delta^{15}N^{bulk}$). Therefore, the variation observed in both studies is much higher compared to the measurements by Harris et al. (2014), where the N_2O isotopic composition deviated only slightly from atmospheric background. A consistent decrease in $\delta^{15}N^{bulk}$ in parallel with increasing N_2O mole fractions (accumulation of soil-derived N_2O) confirms that the soil N_2O source is depleted in ^{15}N-N_2O relative to ambient N_2O (Toyoda et al., 2013). A similar pattern was found for $\delta^{18}O$; an increase in N_2O mole fraction was associated with a decrease in ^{18}O-N_2O, again indicating that soil emissions were depleted in ^{18}O-N_2O with respect to the atmospheric background. In contrast, Harris et al. (2014) reported a decoupling of $\delta^{18}O$ and $\delta^{15}N^{bulk}$. This may have been due to only marginal influence of soil-emitted N_2O since the measurements were carried out in an urban area and approx. 95 m above the ground. Studies on N_2O derived from combustion processes indicate that some of these sources might be less depleted or even enriched in ^{15}N-N_2O compared to ambient N_2O (Harris et al., 2015; Ogawa and Yoshida, 2005).

4.3 Isotopic composition of soil-emitted N_2O

The SP of soil-emitted N_2O observed in our study (1 to 17 ‰) is within the ranges expected for a mixture of the two process groups N_2O_N and N_2O_D and does not necessarily indicate a significant contribution of N_2O reduction, an effect which is discussed further below. Isotopic composition of soil-emitted N_2O has been predominately determined in laboratory incubation studies (Köster et al., 2013a, b; Perez et al., 2006; Well and Flessa, 2009b; Well et al., 2006, 2008). Additionally, results from field experiments using static chambers (Opdyke et al., 2009; Ostrom et al., 2010; Toyoda et al., 2011; Yamulki et al., 2001) and N_2O accumulation below a snowpack have been published (Mohn et al., 2013). Based on pure-culture studies, SP values from 19.7 to 40 and −8.7 to 8.5 ‰, were observed for N_2O_N and N_2O_D, respectively (Decock and Six, 2013b). In field experiments SP was found to range between −1 and 32 ‰ (Opdyke et al., 2009), −3 and 18 ‰ (Yamulki et al., 2001), −14 and 90 ‰ (Toyoda et al., 2011) and 0 and 13 ‰ (Ostrom et al., 2010). The very high SP values detected by Toyoda et al. (2011) may have resulted from extensive N_2O reduction to N_2, a process increasing SP, $\delta^{15}N^{bulk}$ and $\delta^{18}O$ (Ostrom et al., 2007). For $\delta^{15}N^{bulk}$ and $\delta^{18}O$, a much wider variation as compared to SP is expected because these variables depend both on fractionation factors, which vary among different microbial communities and depend on reaction conditions as well as on the isotopic composition of the substrate (Baggs, 2008). Under field conditions, $\delta^{15}N^{bulk}$ was reported to range between −17 and 9 ‰ (Opdyke et al., 2009), −27 and 1 ‰ (Yamulki et al., 2001), −44 and 34 ‰ (Toyoda et al., 2011), and −18 and −15 ‰ (Ostrom et al., 2010), covering the range of −29 to −3 ‰ observed in this study. With respect to $\delta^{18}O$, the values of 22.6 to 34.8 ‰ detected for grassland in this study are at the lower end of measurements under field conditions (4–82 ‰).

4.4 Changes in N_2O source signatures induced by N_2O reduction to N_2

Quantitative source partitioning between process groups N_2O_N and N_2O_D based on SP is possible only when no other processes except those contained in the process groups have an influence on the site-specific N_2O isotopic composition. However, in the terminal step of denitrification, namely the reduction of N_2O to N_2, N–O bonds between lighter isotopes are cleaved preferentially, leading to an increase in SP, $\delta^{15}N^{bulk}$ and $\delta^{18}O$ in the remaining N_2O. Consequently, part of the N_2O originating from a combination of the two process groups, i.e., N_2O_N and N_2O_D, may have been consumed by N_2O-to-N_2 reduction prior to emission.

For the identification of processes determining N_2O isotopic composition, isotopocule maps were suggested on which site preference is plotted versus the difference in substrate and product isotopic composition (Koba et al., 2009). The determination of isotopic composition in the substrates is time consuming and additionally confounded in our study by the large and varying footprint area. Therefore, we present a modified isotope map of SP versus $\delta^{15}N^{bulk}$ (Fig. 7, left panel) instead of $\Delta\delta^{15}N$, the $\delta^{15}N$ differences between substrate and product (i.e., N_2O gas). Rectangles for the process groups N_2O_N and N_2O_D are defined by SP values given by Decock and Six (2013b) and by $\delta^{15}N^{bulk}$ values calculated based on process fractionation factors and substrate isotopic composition. For nitrification and denitrification, minimum and maximum fractionation factors of −90 to −40 ‰ and

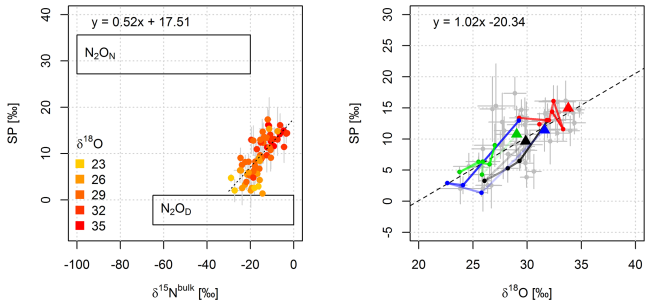

Figure 7. Left panel: map of SP vs. $\delta^{15}N^{bulk}$, with rectangles representing process groups N_2O_N and N_2O_D based on SP values in Decock and Six (2013b), $\delta^{15}N^{bulk}$ estimated from minimum and maximum fractionation factors reported in Baggs (2008), and substrate isotopic compositions reported by Bedard-Haughn et al. (2003), Pörtl et al. (2007) and Toyoda et al. (2011). Right panel: map of SP vs. $\delta^{18}O$ with traces of management events (Mana I in black, Mana II in red, Mana III in green) and the rewetting event (blue). Isotopic compositions are plotted for the transparent blue sections in Fig. 3, including one preceding and one following composition. The preceding composition is represented by the enlarged filled triangle and transparency of the line connecting the composition decreases with event duration.

−40 to −15 ‰ were assumed (Baggs, 2008); for the isotopic compositions of the N_2O precursors (i.e., NH_4^+ and NO_3^-) a range of −20 to +10 and −25 to 15 ‰ were assumed. Koba et al. (2009) attributed a concurrent decrease in $\delta^{15}N^{bulk}$ with increasing SP values as indicative of an increasing contribution of N_2O_N. In contrast, an increase in $\delta^{15}N^{bulk}$ in parallel with increasing SP values (enrichment of ^{15}N in the α position relative to the β position), as observed in the present study, was attributed to a substantial increase in N_2O reduction to N_2. Our results (Fig. 7, left panel) indicate that N_2O is predominately formed by bacterial denitrification and that deviations in the isotope values from denitrification may have been caused by variations in the extent to which N_2O was reduced to N_2. It is noteworthy that, based on such modified isotope maps, systematic changes in $\delta^{15}N^{bulk}$ induced by systematic changes in the N isotopic composition of one of the precursors NH_4^+ or NO_3^- could be misinterpreted as reduction events (Well et al., 2012).

In addition to the SP vs. $\delta^{15}N^{bulk}$ maps, SP vs. $\delta^{18}O$ maps have been suggested to trace N_2O reduction to N_2 (Lewicka-Szczebak et al., 2014, 2015; Well et al., 2012). While $\delta^{15}N^{bulk}$ depends on the isotopic composition of the precursor (e.g., NO_3^-) and, thus, may vary considerably, $\delta^{18}O$-N_2O is expected to be more stable as, during both nitrification and denitrification, oxygen (O) later found in N_2O may almost completely originate from water (Kool et al., 2009). Due to this almost complete O exchange with water, relatively stable $\delta^{18}O$ in soil water, and the observed constant ratio of fractionation factors for SP and $\delta^{18}O$-N_2O ($r_{sp\text{-}o}$), variation in the share of N_2O reduced to N_2 should be reflected in a linear relationship between SP and $\delta^{18}O$-N_2O with a slope of 0.2–0.5 (Jinuntuya-Nortman et al., 2008; Ostrom et al., 2007; Well and Flessa, 2009a). In this study, a linear relationship with a slope of 1.02 was found (Fig. 7, right panel). Tracking the management events (Mana I to Mana III) and the rewetting event in SP vs. $\delta^{18}O$ space revealed that the onset of such an event is associated with a decrease in both SP and $\delta^{18}O$, gradually increasing back to approximately initial values, except for Mana II. During Mana II, no significant change in SP vs. $\delta^{18}O$ occurred (Fig. 7, right panel, red trace). The gradual increase in isotopic composition supports the conclusion from the SP / $\delta^{15}N^{bulk}$ map that N_2O was mainly produced by bacterial denitrification and that variations in isotopic composition may have been caused predominately by N_2O reduction to N_2. This interpretation is in agreement with observations of the isotopic composition of N_2O, NO_3^- and NH_4^+ during a rewetting event in an agricultural field (Decock and Six, 2013a). Additionally, $\delta^{18}O$ was found to be positively correlated with $\delta^{15}N^{bulk}$, which enforces the interpretation that varying shares of N_2O reduction occurred because it acts on both N and O isotopic composition (Koehler et al., 2012).

As stated above, the ratios of fractionation factors for $\delta^{18}O$ and $\delta^{15}N^{bulk}$ ($r_{o\text{-}n}$) and SP and $\delta^{18}O$ ($r_{sp\text{-}o}$) during N_2O reduction were 2.5 and 0.2 to 0.5 in laboratory incubation experiments (Jinuntuya-Nortman et al., 2008; Ostrom et al., 2007; Well and Flessa, 2009a). In our study, $r_{o\text{-}n}$ and $r_{sp\text{-}o}$ were 0.5 and 1, respectively, for the whole data set. We also calculated these ratios for a subset of data for which all δ values (SP, $\delta^{15}N^{bulk}$ and $\delta^{18}O$) increased for 2 consecutive days, indicating that N_2O reduction may have occurred. Such events were observed on eight occasions. If source processes (N_2O_D, N_2O_N) contributed constantly over 2 consecutive measuring days, changes in the isotopic composition of emitted N_2O were solely attributed to changes in the fraction of N_2O reduction. Under such conditions one would expect that the ratio of the changes in $\delta^{18}O$ and $\delta^{15}N^{bulk}$ ($r_{o\text{-}n}$) is around 2.5 and that the ratio of the changes in SP and $\delta^{18}O$ ($r_{sp\text{-}o}$) is between 0.2 and 0.5. The mean (median) ratios for $r_{o\text{-}n}$ and $r_{sp\text{-}o}$ for these selected events were 0.69 (0.44) and 2.1 (1.16), respectively. While the high values of $r_{sp\text{-}o}$ indicate that, for instance, changing physical conditions such as soil moisture may play a role in field measurements, the deviation of $r_{o\text{-}n}$ from the value of 2.5 could either indicate that the fractionation factor for ^{18}O might be smaller than the one for ^{15}N or that there is no correlation of fractionation factors in natural environments. This is in line with recent findings showing that apparent isotope effects associated with N_2O reduction are sensitive to experimental conditions which influenced diffusive isotope effects (Lewicka-Szczebak et al., 2014, 2015). The same study also showed that fractionation factors during N_2O reduction for ^{15}N and ^{18}O were variable (from −11 to +12 ‰ and from −18 to +4 ‰, respectively) and not predictable for field conditions yet. Therefore, to date, the amount of N_2O reduction prior to emission cannot be inferred with sufficient robustness from field measure-

ments alone without the knowledge of the isotopic composition of the substrates.

4.5 Controls on isotopic composition and event-based data aggregation

The high temporal resolution of N_2O isotopic and auxiliary measurements allowed us to investigate the controls on N_2O isotopic composition over the 3-month campaign period. Correlations with isotopic composition were highest and positive for DOC and soil temperature (Table 2). The significant correlation with temperature for the whole campaign was due to a significant correlation during the dry part of the campaign. If the increase in SP was due to an increased contribution of nitrification, $\delta^{15}N^{bulk}$ should decrease due to the higher isotopic fractionation during this process. The simultaneous increase in SP, $\delta^{15}N^{bulk}$ and $\delta^{18}O$ revealed in Fig. 7, however, indicates an increased share of N_2O reduction to N_2, which might have been triggered by increased substrate availability (DOC) for heterotrophic denitrification. The reported effect of temperature on the $N_2O : N_2$ ratio is not entirely certain, but a decrease has been observed with increasing temperature, supporting the hypothesis that N_2O reduction increased as temperature rose throughout the measurement period (Saggar et al., 2013).

Though substrate availability has been identified as a major control on N_2O source processes (see references in Saggar et al., 2013), correlations between N_2O isotopic composition and NO_3^- and NH_4^+ concentrations were low, except for the correlation with $\delta^{15}N^{bulk}$. The reason might be both the number of measurement points for substrate concentrations being lower compared to other explanatory variables and substrate concentrations not necessarily reflecting process or turnover rates (Wu et al., 2012).

The low explanatory power of all linear regressions underlines that drivers of N_2O emissions are highly variable and may even change from event to event. In the absence of management or rewetting events (group BG), isotopic composition covered the whole range of measured values, while management or rewetting events were characterized by lower variability in isotopic composition. Values for SP, $\delta^{15}N^{bulk}$ and $\delta^{18}O$ were low for Mana I, rewetting and Mana III, whereas Mana II showed increased SP, $\delta^{15}N^{bulk}$ and $\delta^{18}O$. This indicates that processes must have been different for Mana II, although management was almost identical.

4.6 Short-term variation in isotopic composition

The Keeling plot approach is based on the conservation of mass and assumes that the atmospheric concentration of a gas in the surface layer is a mixture of background atmospheric concentration and a variable amount of gas added by a source, raising the atmospheric concentration above background. The source's isotope value can be determined, given that its isotope value remains constant during the observation period. In this study, we used noon-to-noon data in the Keeling plots to determine isotope values of soil-derived N_2O for the respective noon-to-noon period. Hence, the source processes underlying these N_2O emissions have to be constant on this timescale. Currently, little is known about the rate of change of N_2O source processes over time steps of minutes to hours. However, changing relative contributions of source processes, which change the isotopic composition in soil-emitted N_2O, would be reflected in deviations from a linear relation between inverse concentration and isotopic composition. As the Keeling plots showed no obvious deviations from a linear relation within our measurement precision (see Supplement S1), we conclude (1) that the use of the Keeling plot approach was valid in our study and (2) that changes in N_2O source processes in our study site occurred at a time step of 1 day or more. While our data suggest that there are little or no changes in source processes underlying N_2O emissions within a noon-to-noon period, clear and distinct day-to-day variation in isotope values of soil-derived N_2O, especially in SP, were observed. Such changes were often strong and abrupt following management events (Mana I and III, Rewetting), indicating a significant response of microbial processes to the imposed disturbance. Larger than expected variability in isotope values was observed between management events (class BG) when no obvious variation in environmental drivers occurred. Since noon-to-noon concentration increases were very small during these periods, part of this variability may be attributed to increased uncertainty around the intercept of the Keeling plot. This is also reflected in the relatively large error bars around isotope values on days when overnight N_2O concentration increases was low (Fig. 3). Alternatively, the variation in isotope values associated with small overnight concentration increase may result from other land use or land cover. The EC fluxes are calculated from the turbulent fluctuation of concentration and vertical wind speed (i.e., the covariance of the concentration and wind speed deviations from the half-hourly mean) and therefore account for the modulation of concentration around a short-term (30 min) mean caused by locally emitted N_2O. Isotopic composition based on Keeling plots, however, is determined from total N_2O accumulated in the nocturnal boundary layer, and, thus, this approach also contains molecules that were emitted outside the flux footprint, which almost exclusively comprised our grassland site (Zeeman et al., 2010), within the larger concentration footprint (Griffis et al., 2007). However, two facts indicate a major influence of the studied grassland on the determined N_2O isotopic composition: First, the N_2O isotopic composition is very stable for a noon-to-noon period as indicated by a linear relationship between individual measurements (Supplement S1). This relationship persists even though wind speed and direction change and, therefore, individual N_2O isotope measurements integrate over a 16-min sampling interval originate from different source areas. Secondly, the CHA grassland can be characterized as a site with vigor-

ous N_2O emission, and therefore may dominate the determined N_2O isotopic composition, as the influence of a source area increment scales with the source strength. The grassland site was restored in 2012, which led to an extraordinarily high N_2O-N emission of 29.1 kg ha^{-1} year^{-1} (Merbold et al., 2014). In the following year 2.5 kg N_2O-N ha^{-1} were released. This value is still in the range of maximum emissions reported for a different intensively managed Swiss grassland site, emitting 1.5–2.6 kg N ha^{-1} year^{-1}, and at least a factor of 5 greater compared to an extensively managed grassland site with less than 0.5 kg N ha^{-1} year^{-1} (Ammann et al., 2009). With regard to distant land use and land cover, the 2.5 kg N_2O-N is also more than double the median (between the 70th and 75th percentile) of all reported values for cultivated temperate sites and is higher than the highest value reported for forests presented in a study containing 1008 N_2O emission measurements from agricultural fields (Stehfest and Bouwman, 2006). However, the possibility cannot be excluded that the N_2O isotopic signatures analyzed above the grassland site were influenced by adjacent ecosystems.

4.7 Flux-weighted averages of source isotopic compositions

N_2O isotopic composition can be used to calculate and further constrain the global N_2O budget (Kim and Craig, 1993; Yoshida and Toyoda, 2000). The analysis of emissions from different sources such as agricultural soils or managed grassland based on box models and isotopic composition is complicated by the distinct temporal and spatial variability of isotopic composition (Kim and Craig, 1993; Toyoda et al., 2011; Yoshida and Toyoda, 2000); hence, flux-weighted averages are required to obtain representative values for agricultural N_2O (Perez et al., 2001). Our flux-weighted averages of 6.9 ± 4.3, -17.4 ± 6.2 and 27.4 ± 3.6 ‰ for SP, $\delta^{15}N^{bulk}$ and $\delta^{18}O$ are well within the range of the values of 2.9 to 36.6, -41.5 to -1.9 and 23.2 to 51.7 ‰ for agricultural soils (Park et al., 2011; Toyoda et al., 2011). The comparison with other grassland soils (Opdyke et al., 2009; Park et al., 2011) indicates that the variability of isotopic composition within a group, such as grassland, may be considerable (for SP: 2.2 to 11.1 ‰). One has to keep in mind, however, that part of the observed variability may be attributed to the fact that the footprint area of the N_2O isotopic composition includes areas with other land use or land cover. Another part of the variability might also be explained by a limited compatibility of different laboratory results, as recently demonstrated in an inter-laboratory comparison campaign (Mohn et al., 2014). The uncertainty in budgets derived by isotopic composition depends on the uncertainty of the representative isotopic composition for a single source, which can be reduced by a quasi-continuous measurement approach, as shown in this study.

5 Conclusions

Our field observations indicate that nitrifier-denitrification and denitrification (process group N_2O_D) dominated throughout the measurement period and that variation in isotopic composition was more likely due to variation in the extent of N_2O reduction rather than contributions of NH_2OH oxidation or fungal denitrification. A high temporal resolution of isotopic composition in soil-emitted N_2O showed that, at the beginning of the growing season, medium wfps and low temperature induced low isotope values (representative for process group N_2O_D), whereas in the second part of the measurement period, higher temperature and DOC stimulated N_2O reduction to N_2, although wfps was lower. Management or rewetting events were mostly characterized by low SP, $\delta^{15}N^{bulk}$ and $\delta^{18}O$, but the event Mana II indicated that processes underlying N_2O emissions can vary even under similar management conditions. With this study, a new method is available that can provide real-time data sets for various individual N_2O-emitting (eco)systems, such as grassland or agricultural soils, which will help in further constraining the global N_2O budget based on box model calculations. However, future campaigns should be accompanied by footprint modeling in order to optimize of the inlet height and associated concentration footprint size.

The Supplement related to this article is available online at doi:10.5194/bg-12-2517-2015-supplement.

Acknowledgements. We are grateful to Hans-Ruedi Wettstein and his team for the collaboration with the ETH research station Chamau and Christoph Zellweger for support with the determination of GHG mixing ratios in our target gases. Antoine Roth is acknowledged for his support during the field campaign. This project was funded by the State Secretariat for Education and Research (SER) within COST Action ES0806. The QCLAS used for EC measurements was funded by the R'Equip Project (206021 133763) of the Swiss National Science Foundation. Funding form GHG-Europe (FP7, EU contract no. 244122) and COST Action ES0804–ABBA is gratefully acknowledged. Instrumental developments at Empa were supported by the Swiss National Science Foundation (SNSF). Technical support on the eddy-covariance station has been provided by Thomas Baur and Peter Plüss. The preparation of N_2O isotope standards and inter-laboratory comparison measurements were supported by the EMRP ENV52 project "Metrology for high-impact greenhouse gases". The EMRP is jointly funded by the EMRP participating countries within EURAMET and the European Union.

Edited by: A. Neftel

References

Ammann, C., Spirig, C., Leifeld, J., and Neftel, A.: Assessment of the nitrogen and carbon budget of two managed temperate grassland fields, Agr. Ecosyst. Environ., 133, 150–162, 2009.

Baggs, E. M.: A review of stable isotope techniques for N_2O source partitioning in soils?: recent progress, remaining challenges and future considerations, Rapid Commun. Mass Spectr., 22, 1664–1672, 2008.

Baldocchi, D. and Meyers, T.: On using eco-physiological, micrometeorological and biogeochemical theory to evaluate carbon dioxide, water vapor and trace gas fluxes over vegetation: a perspective, Agr.. For. Meteorol., 90, 1–25, 1998.

Bedard-Haughn, A., van Groenigen, J. W., and van Kessel, C.: Tracing ^{15}N through landscapes: potential uses and precautions, J. Hydrol., 272, 175–190, 2003.

Butterbach-Bahl, K., Baggs, E. M., Dannenmann, M., Kiese, R., and Zechmeister-Boltenstern, S.: Nitrous oxide emissions from soils: how well do we understand the processes and their controls?, Philos. Trans. R. Soc. B-Biological Sci., 368, 20130122, doi:10.1098/rstb.2013.0122, 2013.

Davidson, E. A.: The contribution of manure and fertilizer nitrogen to atmospheric nitrous oxide since 1860, Nat. Geosci., 2, 659–662, 2009.

Decock, C. and Six, J.: An assessment of N-cycling and sources of N_2O during a simulated rain event using natural abundance ^{15}N, Agr.., Ecosyst. Environ., 165, 141–150, 2013a.

Decock, C. and Six, J.: How reliable is the intramolecular distribution of ^{15}N in N_2O to source partition N_2O emitted from soil?, Soil Biol. Biochem., 65, 114–127, 2013b.

Eugster, W. and Plüss, P.: A fault-tolerant eddy covariance system for measuring CH_4 fluxes, Agr. Forest Meteorol., 150, 841–851, 2010.

Griffis, T. J., Zhang, J., Baker, J. M., Kljun, N., and Billmark, K.: Determining carbon isotope signatures from micrometeorological measurements: Implications for studying biosphere–atmosphere exchange processes, Bound.-Lay. Meteorol., 123, 295–316, 2007.

Groffman, P. M., Altabet, M. A., Bohlke, J. K., Butterbach-Bahl, K., David, M. B., Firestone, M. K., Giblin, A. E., Kana, T. M., Nielsen, L. P., and Voytek, M. A.: Methods for measuring denitrification: Diverse approaches to a difficult problem, Ecol. Appl., 16, 2091–2122, 2006.

Harris, E., Nelson, D. D., Olszewski, W., Zahniser, M., Potter, K. E., McManus, B. J., Whitehill, A., Prinn, R. G., and Ono, S.: Development of a Spectroscopic Technique for Continuous Online Monitoring of Oxygen and Site-Specific Nitrogen Isotopic Composition of Atmospheric Nitrous Oxide, Anal. Chem., 86, 1726–1734, doi:10.1021/ac403606u, 2014.

Harris, E., Zeyer, K., Kegel, R., Müller, B., Emmenegger, L., and Mohn, J.: Nitrous oxide emissions and isotopic composition from waste incineration in Switzerland, Waste Manag., 35, 135–140, 2015.

Heil, J., Wolf, B., Brüggemann, N., Emmenegger, L., Tuzson, B., Vereecken, H., and Mohn, J.: Site-specific ^{15}N isotopic signatures of abiotically produced N_2O, Geochim. Cosmochim. Ac., 139, 72–82, 2014.

Jinuntuya-Nortman, M., Sutka, R. L., Ostrom, P. H., Gandhi, H., and Ostrom, N. E.: Isotopologue fractionation during microbial reduction of N_2O within soil mesocosms as a function of water-filled pore space, Soil Biol. Biochem., 40, 2273–2280, 2008.

Keeling, C. D.: The concentration and isotopic abundances of atmospheric carbon dioxide in rural areas, Geochim. Cosmochim. Ac., 13, 322–334, 1958.

Kim, K. R. and Craig, H.: Nitrogen-15 and oxygen-18 characteristics of nitrous oxide: a global perspective, Science, 262, 1855–1857, 1993.

Koba, K., Osaka, K., Tobari, Y., Toyoda, S., Ohte, N., Katsuyama, M., Suzuki, N., Itoh, M., Yamagishi, H., Kawasaki, M., Kim, S. J., Yoshida, N., and Nakajima, T.: Biogeochemistry of nitrous oxide in groundwater in a forested ecosystem elucidated by nitrous oxide isotopomer measurements, Geochim. Cosmochim. Ac., 73, 3115–3133, 2009.

Koehler, B., Corre, M. D., Steger, K., Well, R., Zehe, E., Sueta, J. P., and Veldkamp, E.: An in-depth look into a tropical lowland forest soil: nitrogen-addition effects on the contents of N_2O, CO_2 and CH_4 and N_2O isotopic signatures down to 2-m depth, Biogeochemistry, 111, 695–713, 2012.

Kool, D. M., Wrage, N., Oenema, O., Harris, D., and Van Groenigen, J. W.: The ^{18}O signature of biogenic nitrous oxide is determined by O exchange with water, Rapid Commun. Mass Spectr., 23, 104–108, 2009.

Köster, J. R., Cárdenas, L., Senbayram, M., Bol, R., Well, R., Butler, M., Mühling, K. H., and Dittert, K.: Rapid shift from denitrification to nitrification in soil after biogas residue application as indicated by nitrous oxide isotopomers, Soil Biol. Biochem., 43, 1671–1677, 2011.

Köster, J. R., Well, R., Dittert, K., Giesemann, A., Lewicka-Szczebak, D., Mühling, K.-H., Herrmann, A., Lammel, J., and Senbayram, M.: Soil denitrification potential and its influence on N_2O reduction and N_2O isotopomer ratios, Rapid Commun. Mass Spectr., 27, 2363–73, 2013a.

Köster, J. R., Well, R., Tuzson, B., Bol, R., Dittert, K., Giesemann, A., Emmenegger, L., Manninen, A., Cárdenas, L., and Mohn, J.: Novel laser spectroscopic technique for continuous analysis of N_2O isotopomers–application and intercomparison with isotope ratio mass spectrometry, Rapid Commun. Mass Spectr., 27, 216–22, 2013b.

Lewicka-Szczebak, D., Well, R., Köster, J. R., Fuß, R., Senbayram, M., Dittert, K., and Flessa, H.: Experimental determinations of isotopic fractionation factors associated with N_2O production and reduction during denitrification in soils, Geochim. Cosmochim. Ac., 134, 55–73, 2014.

Lewicka-Szczebak, D., Well, R., Bol, R., Gregory, A. S., Matthews, G. P., Misselbrook, T., Whalley, W. R., and Cardenas, L. M.: Isotope fractionation factors controlling isotopocule signatures of soil-emitted N_2O produced by denitrification processes of various rates, Rapid Commun. Mass Spectr.., 29, 269–282, 2015.

Merbold, L., Eugster, W., Stieger, J., Zahniser, M., Nelson, D., and Buchmann, N.: Greenhouse gas budget (CO_2 , CH_4 and N_2O) of intensively managed grassland following restoration, Glob. Change Biol., 20, 1913–1928, 2014.

Mohn, J., Guggenheim, C., Tuzson, B., Vollmer, M. K., Toyoda, S., Yoshida, N., and Emmenegger, L.: A liquid nitrogen-free preconcentration unit for measurements of ambient N_2O isotopomers by QCLAS, Atmos. Meas. Tech., 3, 609–618, doi:10.5194/amt-3-609-2010, 2010.

Mohn, J., Tuzson, B., Manninen, A., Yoshida, N., Toyoda, S., Brand, W. A., and Emmenegger, L.: Site selective real-time measurements of atmospheric N_2O isotopomers by laser spectroscopy, Atmos. Meas. Tech., 5, 1601–1609, doi:10.5194/amt-5-1601-2012, 2012.

Mohn, J., Steinlin, C., Merbold, L., Emmenegger, L., and Hagedorn, F.: N_2O emissions and source processes in snow-covered soils in the Swiss Alps, Isotopes Environ. Health Stud., 49, 520–531, 2013.

Mohn, J., Wolf, B., Toyoda, S., Lin, C. T., Liang, C. M., Brüggemann, N., Wissel, H., Steiker, A. E., Dyckmans, J., Szwek, L., Ostrom, N. E., Casciotti, K. L., Forbes, M., Giesemann, A., Well, R., Doucett, R. R., Yarnes, C. T., Ridley, A. R., Kaiser, J., and Yoshida, N.: Inter-Laboratory assessment of notrous oxide isotopomer analysis of isotopomer analysis by isotope ratio mass spectrometry and laser spectroscopy: current status and perspectives, Rapid Commun. Mass Spectr.., 28, 1995–2007, 2014.

Mosier, A., Kroeze, C., Nevison, C., Oenema, O., Seitzinger, S., and van Cleemput, O.: Closing the global N_2O budget: nitrous oxide emissions through the agricultural nitrogen cycle – OECD/IPCC/IEA phase II development of IPCC guidelines for national greenhouse gas inventory methodology, Nutr. Cycl. Agroecosys., 52, 225–248, 1998.

Myhre, G., Shindell, D., Bréon, F.-M., Collins, W., Fuglestvedt, J., Huang, J., Koch, D., Lamarque, L., Mendoza, B., Nakaijima, T., Robock, A., Stephens, G., Takemura, T., and Zhang, H.: Anthropogenic and Natural Radiative Forcing, in: Climate Change 2013: The Physical Science Basis. Contribution of Working Group I to the Fifth Assessment Report of the Intergovernmental Panel on Climate Change, edited by: Stocker, T., Qin, D., Plattner, G. K., Tignor, M., Allen, S., Boschung, J., Nauels, A., Xia, Y., Bex, V., and Midgley, P., Cambridge University Press, Cambridge, UK and New York, NY, USA, 659–740, 2013.

Ogawa, M. and Yoshida, N.: Intramolecular distribution of stable nitrogen and oxygen isotopes of nitrous oxide emitted during coal combustion, Chemosphere, 61, 877–87, 2005.

Opdyke, M. R., Ostrom, N. E., and Ostrom, P. H.: Evidence for the predominance of denitrification as a source of N_2O in temperate agricultural soils based on isotopologue measurements, Global Biogeochem. Cy., 23, GB4018, doi:10.1029/2009GB003523, 2009.

Ostrom, N. E. and Ostrom, P. H.: The Isotopomers of Nitrous Oxide: Analytical Considerations and Application to Resolution of Microbial Production Pathways, in: Handbook of Envirionmental Isotope Geochemistry Volume 1, edited by: Baskaran, M., Springer Berlin Heidelberg, Berlin, Heidelberg, 453–476, 2011.

Ostrom, N. E., Pitt, A., Sutka, R. L., Ostrom, P. H., Grandy, A. S., Huizinga, K. M., and Robertson, G. P.: Isotopologue effects during N_2O reduction in soils and in pure cultures of denitrifiers, J. Geophys. Res., 112, 1–12, 2007.

Ostrom, N. E., Sutka, R. L., Ostrom, P. H., Grandy, A. S., Huizinga, K. M., Gandhi, H., von Fischer, J. C., and Robertson, G. P.: Isotopologue data reveal bacterial denitrification as the primary source of N_2O during a high flux event following cultivation of a native temperate grassland, Soil Biol. Biochem., 42, 499–506, 2010.

Park, S., Pérez, T., Boering, K. A., Trumbore, S. E., Gil, J., Marquina, S., and Tyler, S. C.: Can N_2O stable isotopes and isotopomers be useful tools to characterize sources and microbial pathways of N_2O production and consumption in tropical soils?, Global Biogeochem. Cy., 25, 1–16, 2011.

Pataki, D., Ehleringer, J., Flanagan, L., Yakir, D., Bowling, D., Still, C., Buchmann, N., Kaplan, J., and Berry, J.: The application and interpretation of Keeling plots in terrestrial carbon cycle research, Global Biogeochem. Cy., 17, 1022, doi:10.1029/2001GB001850, 2003.

Perez, T., Trumbore, S. E., Tyler, S. C., Matson, P. A., Ortiz-Monasterio, I., Rahn, T., and Griffith, D. W. T.: Identifying the agricultural imprint on the global N_2O budget using stable isotopes, J. Geophys. Res., 106, 9869–9878, 2001.

Perez, T., Garcia-Montiel, D. C., Trumbore, S. E., Tyler, S., de Camargo, P. B., Moreira, M., Piccolo, M. C., and Cerri, C.: Nitrous Oxide Nitrification and Denitrification ^{15}N Enrichment Factros from Amazon Forest Soils, Ecol. Appl., 16, 2153–2167, 2006.

Ravishankara, A. R., Daniel, J. S., and Portmann, R. W.: Nitrous oxide (N_2O): the dominant ozone-depleting substance emitted in the 21st century, Science, 80, 123–125, 2009.

Roth, K.: Bodenkartierung und GIS-basierte Kohlenstoffinventur von Graslandböden, University of Zürich (UZH), 132 pp., 2006.

Saggar, S., Jha, N., Deslippe, J., Bolan, N. S., Luo, J., Giltrap, D. L., Kim, D.-G., Zaman, M., and Tillman, R. W.: Denitrification and $N_2O:N_2$ production in temperate grasslands: processes, measurements, modelling and mitigating negative impacts, Sci. Total Environ., 465, 173–195, 2013.

Stehfest, E. and Bouwman, L.: N_2O and NO emission from agricultural fields and soils under natural vegetation: summarizing available measurement data and modeling of global annual emissions, Nutr. Cycl. Agroecosys., 74, 207–228, 2006.

Sutka, R. L., Ostrom, N. E., Ostrom, P. H., Gandhi, H., and Breznak, J. A: Nitrogen isotopomer site preference of N_2O produced by Nitrosomonas europaea and Methylococcus capsulatus Bath, Rapid Commun. Mass Spectr.., 17, 738–45, 2003.

Sutka, R. L., Ostrom, N. E., Ostrom, P. H., Breznak, J. A., Pitt, A. J., Li, F., and Gandhi, H.: Distinguishing Nitrous Oxide Production from Nitrification and Denitrification on the Basis of Isotopomer Abundances, Appl. Environ. Microbiol., 72, 638–644, 2006.

Sutka, R. L., Adams, G. C., Ostrom, N. E., and Ostrom, P. H.: Isotopologue fractionation during N_2O production by fungal denitrification, Rapid Commun. Mass Spectr.., 22, 3989–3996, 2008.

Syakila, A. and Kroeze, C.: The global nitrous oxide budget revisited, Greenh. Gas Meas. Manag., 1, 17–26, 2011.

Toyoda, S. and Yoshida, N.: Determination of Nitrogen Isotopomers of Nitrous Oxide on a Modified Isotope Ratio Mass Spectrometer, Anal. Chem., 71, 4711–4718, 1999.

Toyoda, S., Mutobe, H., Yamagishi, H., Yoshida, N., and Tanji, Y.: Fractionation of N_2O isotopomers during production by denitrifier, Soil Biol. Biochem., 37, 1535–1545, 2005.

Toyoda, S., Yano, M., Nishimura, S., Akiyama, H., Hayakawa, A., Koba, K., Sudo, S., Yagi, K., Makabe, A., Tobari, Y., Ogawa, N. O., Ohkouchi, N., Yamada, K., and Yoshida, N.: Characterization and production and consumption processes of N_2O emitted from temperate agricultural soils determined via isotopomer ratio analysis, Global Biogeochem. Cy., 25, 1–17, 2011.

Toyoda, S., Kuroki, N., Yoshida, N., Ishijima, K., Tohjima, Y., and Machida, T.: Decadal time series of tropospheric abundance of N_2O isotopomers and isotopologues in the Northern Hemisphere obtained by the long-term observation at Hateruma Island, Japan, J. Geophys. Res.-Atmos., 118, 3369–3381, 2013.

Tuzson, B., Zeyer, K., Steinbacher, M., McManus, J. B., Nelson, D. D., Zahniser, M. S., and Emmenegger, L.: Selective measurements of NO, NO_2 and NO_y in the free troposphere using quantum cascade laser spectroscopy, Atmos. Meas. Tech., 6, 927–936, doi:10.5194/amt-6-927-2013, 2013.

Waechter, H., Mohn, J., Tuzson, B., Emmenegger, L., and Sigrist, M. W.: Determination of N_2O isotopomers with quantum cascade laser based absorption spectroscopy, Opt. Express, 16, 9239–9244, 2008.

Watts, S. H. and Seitzinger, S. P.: Denitrification rates in organic and mineral soils from riparian sites?: a comparison of N_2 flux and acetylene inhibition methods, Soil Biol. Biochem., 32, 1383–1392, 2000.

Well, R. and Flessa, H.: Isotopologue enrichment factors of N_2O reduction in soils, Rapid Commun. Mass Spectr., 23, 2996–3002, 2009a.

Well, R. and Flessa, H.: Isotopologue signatures of N2O produced by denitrification in soils, J. Geophys. Res., 114, 1–11, 2009b.

Well, R., Kurganova, I., Lopesdegerenyu, V., and Flessa, H.: Isotopomer signatures of soil-emitted N_2O under different moisture conditions – A microcosm study with arable loess soil, Soil Biol. Biochem., 38, 2923–2933, 2006.

Well, R., Flessa, H., Xing, L., Xiaotang, J., and Römheld, V.: Isotopologue ratios of N_2O emitted from microcosms with NH_4^+ fertilized arable soils under conditions favoring nitrification, Soil Biol. Biochem., 40, 2416–2426, 2008.

Well, R., Eschenbach, W., Flessa, H., von der Heide, C., and Weymann, D.: Are dual isotope and isotopomer ratios of N_2O useful indicators for N_2O turnover during denitrification in nitrate-contaminated aquifers?, Geochim. Cosmochim. Ac., 90, 265–282, 2012.

Wrage, N., Velthof, G. L., van Beusichem, M. L., and Oenema, O.: Role of nitrifier denitrification in the production of nitrous oxide, Soil Biol. Biochem., 33, 1723–1732, 2001.

Wu, H., Dannenmann, M. D., Wolf, B., Han, X. G., Zheng, X., and Butterbach-Bahl, K.: Seasonality of soil microbial nitrogen turnover in continental steppe soils of Inner Mongolia, Ecosphere, 3, 34, doi:10.1890/ ES11-00188.1, 2012.

Wunderlin, P., Mohn, J., Joss, A., Emmenegger, L., and Siegrist, H.: Mechanisms of N_2O production in biological wastewater treatment under nitrifying and denitrifying conditions, Water Res., 46, 1027–37, 2012.

Wunderlin, P., Lehmann, M. F., Siegrist, H., Tuzson, B., Joss, A., Emmenegger, L., and Mohn, J.: Isotope signatures of N_2O in a mixed microbial population system: constraints on N_2O producing pathways in wastewater treatment, Environ. Sci. Technol., 47, 1339–1348, 2013.

Yamulki, S., Toyoda, S., Yoshida, N., Veldkamp, E., Grant, B., and Bol, R.: Diurnal fluxes and the isotopomer ratios of N_2O in a temperate grassland following urine amendment, Rapid Commun. Mass Spectr.., 15, 1263–1269, 2001.

Yoshida, N. and Toyoda, S.: Constraining the atmospheric N_2O budget from intramolecular site preference in N_2O isotopomers, Nature, 405, 330–334, 2000.

Zeeman, M., Hiller, R., Gilgen, A. K., Michna, P., Plüss, P., Buchmann, N., and Eugster, W.: Management and climate impacts on net CO_2 fluxes and carbon budgets of three grasslands along an elevational gradient in Switzerland, Agr. Forest Meteorol., 150, 519–530, 2010.